Supplementary Information

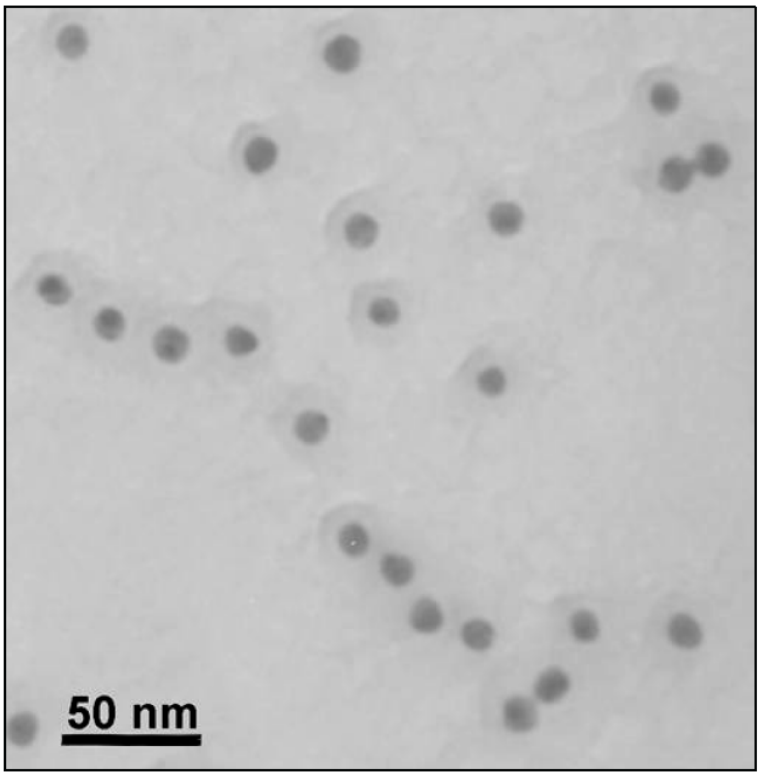

Fig. S1 Transmission electron microscopy (TEM) image of BSA-protected R6G/MPA-Au NPs.

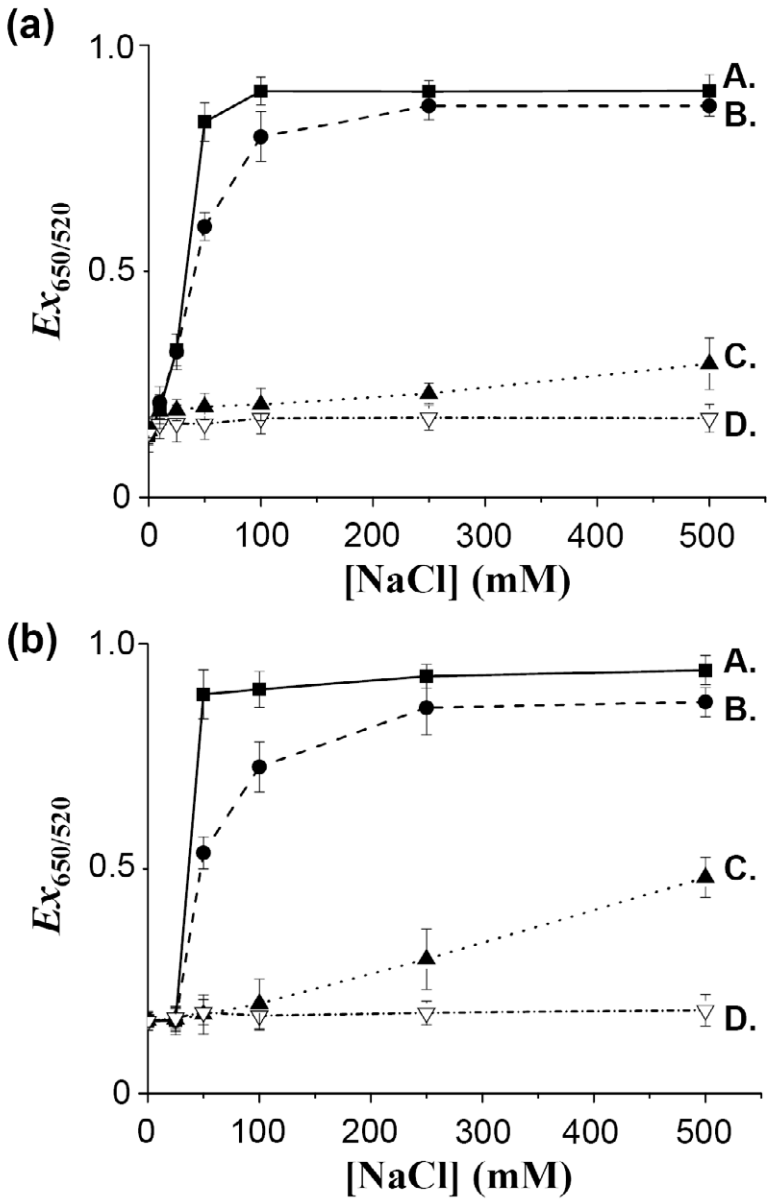

Fig. S2 Effect of the concentration ratio of BSA to Au NPs ([BSA]/[Au NPs]) on the stability of the (a) R6G/MPA-Au NPs@BSA (0.6 nM) and (b) 2-ME/$S_2O_3^{2-}$-Au NPs@BSA (1.5 nM) in 5 mM sodium phosphate (pH 5.0) and 5 mM glycine-NaOH (pH 10.0) buffer containing NaCl (0–500 mM), respectively. The [BSA]/[Au NPs] ratios in (a) were (A) 0, (B) 10, (C) 100, and (D) 1000; in (b) they were (A) 0, (B) 10, (C) 50, and (D) 100. Error bars are standard deviation values across four repetitive experiments.

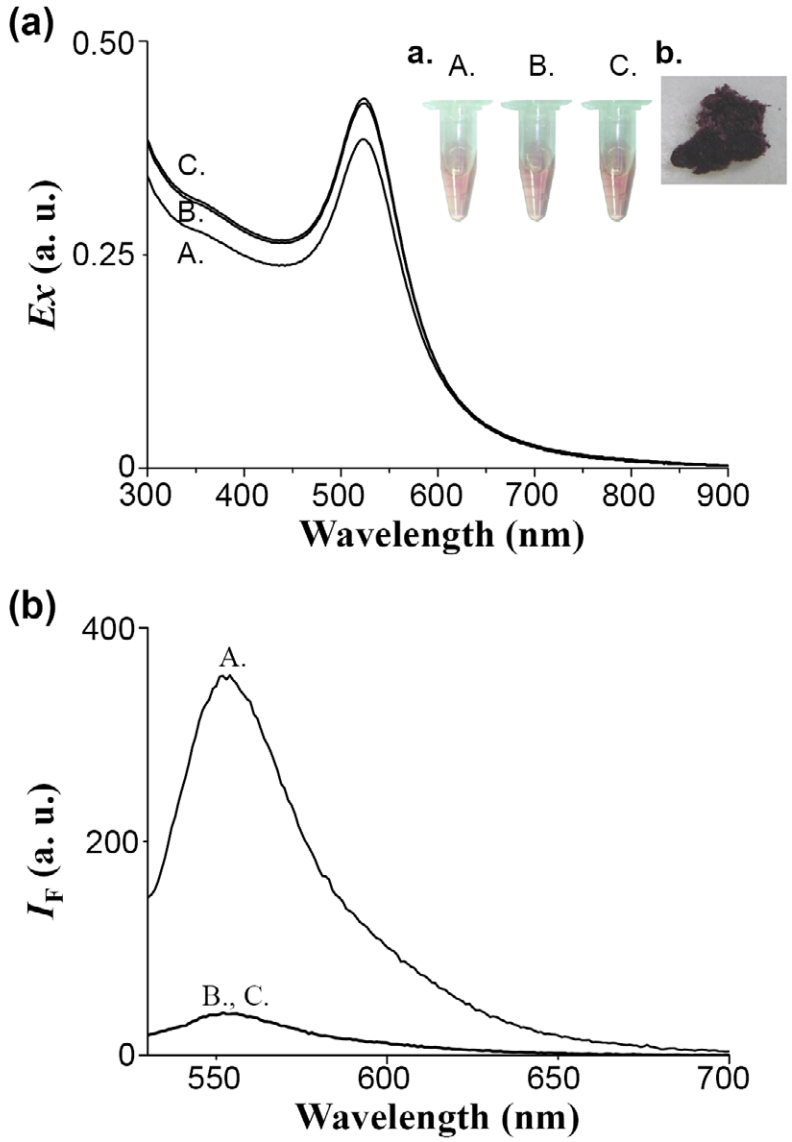

Fig. S3 (a) UV–vis absorption spectra of (A) Au NPs (3.0 nM), (B) R6G/MPA-Au NPs@BSA (3.0 nM), and (C) a re-suspended lyophilized powder of R6G/MPA-Au NPs@BSA (3.0 nM) in 5 mM sodium phosphate (pH 5.0) solution. Inset a: Photographic images of the Au NP solutions. Inset b: Photograph of the lyophilized powder of R6G/MPA-Au NPs@BSA. (b) Fluorescence spectra of (A) R6G (300 nM), (B) R6G/MPA-Au NPs@BSA (3.0 nM), and (C) a re-suspended lyophilized powder of R6G/MPA-Au NPs@BSA (3.0 nM) in 5 mM sodium phosphate (pH 5.0). Other conditions were the same as those described in Fig. S2.

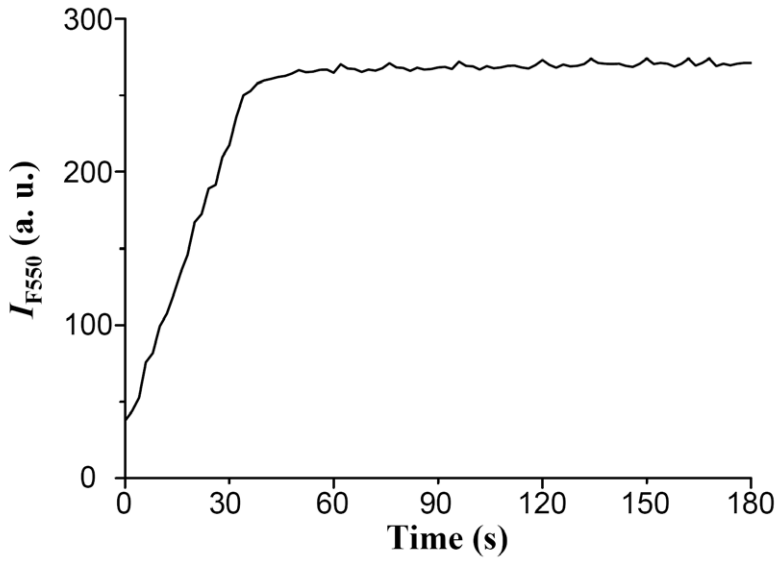

Fig. S4 Time course measurement of fluorescence intensity at 550 nm (I_{F550}) for R6G/MPA-Au NPs@BSA upon the addition of Hg^{2+} (10 μM). Other conditions were the same as those described in Fig. 1.

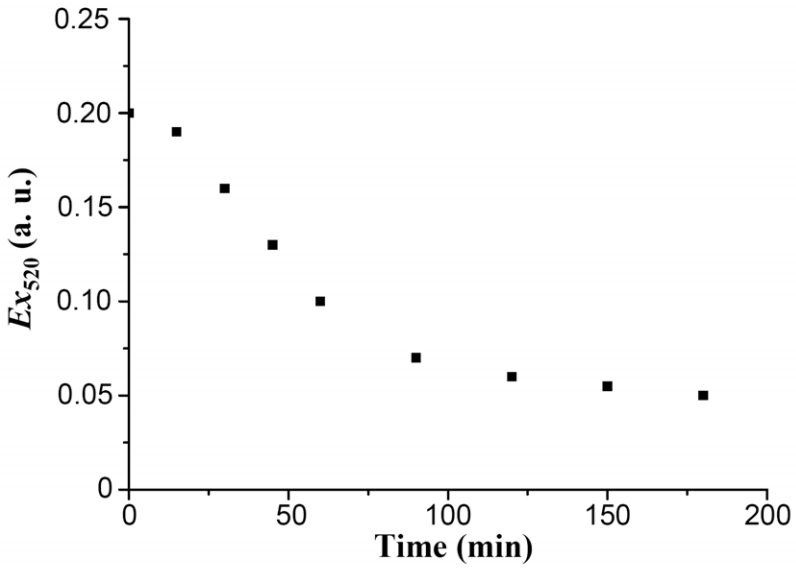

Fig. S5 Time-course measurement of the values of extinction coefficients at 520 nm (Ex_{520}) of the 2-ME/$S_2O_3^{2-}$-Au NPs@BSA in the presence of Pb^{2+} (1.0 μM). Other conditions were the same as those described in Fig. 2.

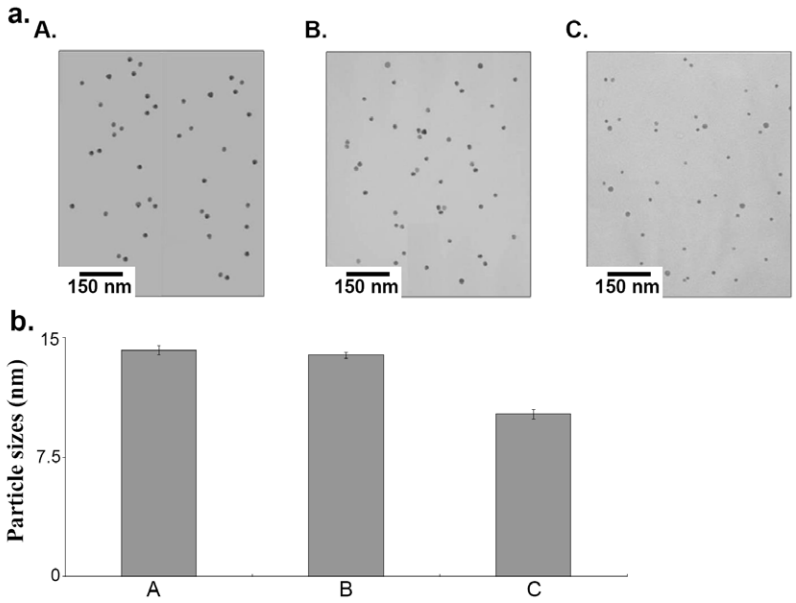

Fig. S6 (a) Transmission electron microscopy (TEM*)* images and (b) average particle sizes of the (A) BSA-capped Au NPs, (B) 2-ME/$S_2O_3^{2-}$-Au NPs@BSA, and (C) 2-ME/$S_2O_3^{2-}$-Au NPs@BSA and $PbCl_2$ (1.0 μM). The average particle sizes were obtained from counts of 100 particles in the TEM images. Other conditions were the same as those described in Fig. 2.

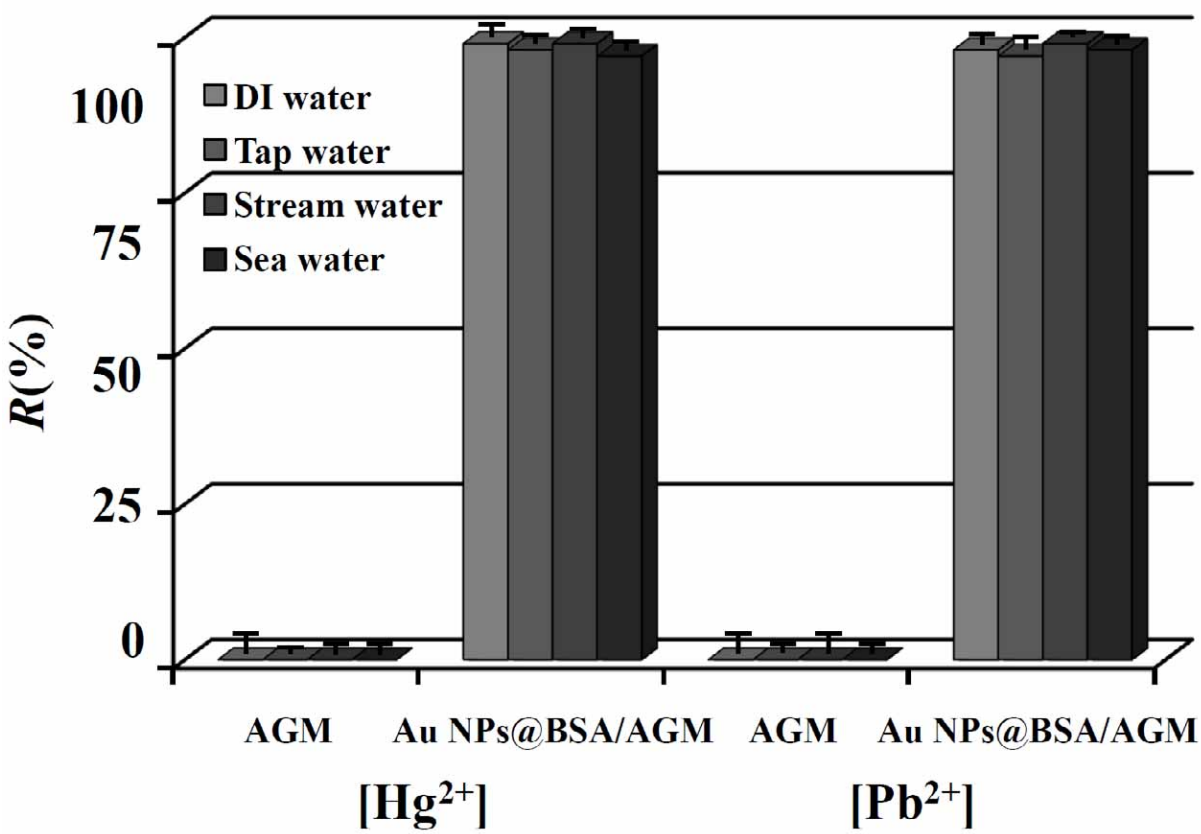

Fig. S7 Removal efficiency (R) of Hg^{2+} ions (1 μM) or Pb^{2+} ions (1 μM) in 10 mL DI water or 2-fold diluted tap, stream or sea waters by bared agarose gel membrane (AGM) or Au NPs@BSA-trapped agarose gel membrane (Au NPs@BSA/AGM). The percentage of metal ions removed by the adsorbents was calculated as follows: $R(\%) = (M_0 - M_{eq})/M_0 \times 100$, where R is the removal efficiency of the metals ions, M_0 is the initial ion concentration, and M_{eq} is the ion concentration at equilibrium.

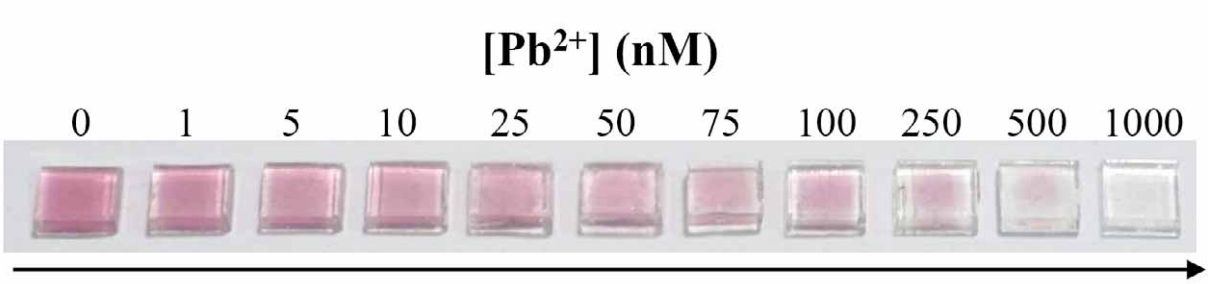

Fig. S8 The colors of 2-ME/$S_2O_3^{2-}$-Au NPs@BSA/AGM probe for detection of Pb^{2+} ions (0 − 1 μM). Other conditions were the same as those described in Fig. 6a.